Role of the Cytoplasmic Domain in *Anabaena* Sensory Rhodopsin Photocycling: Vectoriality of Schiff Base Deprotonation

Oleg A. Sineshchekov,*† Elena N. Spudich,* Vishwa D. Trivedi,* and John L. Spudich*
*Center for Membrane Biology, Department of Biochemistry and Molecular Biology, University of Texas Medical School, Houston, Texas; and †Biology Department, Moscow State University, Vorobievy Gory, Moscow, Russia

ABSTRACT Light-induced electric signals in intact *Escherichia coli* cells generated by heterologously expressed full-length and C-terminally truncated versions of *Anabaena* sensory rhodopsin (*A*SR) demonstrate that the charge movements within the membrane-embedded part of the molecule are stringently controlled by the cytoplasmic domain. In particular, truncation inverts the direction of proton movement during Schiff base deprotonation from outward to cytoplasmic. Truncation also alters faster charge movements that occur before Schiff base deprotonation. Asp^{217} as previously shown by FTIR serves as a proton acceptor in the truncated *A*SR but not in the full-length version, and its mutation to Asn restores the natural outward direction of proton movement. Introduction of a potential negative charge (Ser^{86} to Asp) on the cytoplasmic side favors a cytoplasmic direction of proton release from the Schiff base. In contrast, mutation of the counterion Asp^{75} to Glu reverses the photocurrent to the outward direction in the truncated pigment, and in both truncated and full-length versions accelerates Schiff base deprotonation more than 10-fold. The communication between the cytoplasmic domain and the membrane-embedded photoactive site of *A*SR demonstrated here is likely to derive from the receptor's use of a cytoplasmic protein for signal transduction, as has been suggested previously from binding studies.

INTRODUCTION

Rhodopsins constitute a large diverse group of membrane-embedded retinylidene proteins with seven transmembrane segments found throughout organisms ranging from bacteria to humans (1–4). Based on their primary structures, spatial arrangements of their helices, and configurations of their retinal chromophores, rhodopsins fall into two classes. Type 1 rhodopsins function as ion pumps to capture light energy (5,6) or as light receptors in sensory transduction pathways in prokaryotic and eukaryotic microorganisms (7). Type 2 rhodopsins are light sensors in visual systems and function as G-protein–coupled receptors (8). In both types, seven transmembrane α-helices form a pocket for the retinal chromophore buried in the membrane-embedded domain of the protein. The retinal is attached in a protonated Schiff base linkage to a lysine residue in the seventh helix. In proton-pumping rhodopsins, microbial sensory rhodopsins, and visual pigments, photoisomerization of retinal causes transfer of the Schiff base proton to proton acceptors on the protein. The deprotonation of the retinylidene Schiff base causes a large blue-shift in the pigment, thereby generating a spectrally distinct intermediate called the M intermediate in type 1 rhodopsins and Meta-II in visual pigments. The M and Meta-II intermediates are signaling states of sensory rhodopsins, and M is also a critical intermediate in the proton-pumping rhodopsins.

Type 1 microbial rhodopsins so far characterized differ from type 2 visual pigments in the importance of the C-terminal extension of the proteins, which protrudes from the cytoplasmic end of the seventh helix into the cytoplasm. In the well-characterized mammalian rod visual pigment, the C-terminal extension is an active participant in the signal transduction process, and its modification alters the photochemical properties and biochemical functions of the protein (8,9). In contrast, early studies of the first discovered type 1 proteins, the haloarchaeal proton pump bacteriorhodopsin and phototaxis receptors sensory rhodopsins I and II (SRI and SRII), established that their flexible cytoplasmic C-terminal domains could be truncated or modified without loss of function (10–12). Removal of this flexible ''tail'' has been advantageous. Truncation of the C-terminus greatly increased expression levels of SRI (13). Furthermore, truncation of the dispensable C-terminal extensions favors crystallization by eliminating a flexible domain.

A large number of new type 1 rhodopsins have been identified by microbial genomics during the last few years (14), which are predicted to be in some cases light-driven ion transporters and in others, photosensors. A striking diversity in photochemistry and mechanisms of signal transduction has been observed among the photosensors (7), for which the sensory function has been proven (15–17) or predicted (18,19). *Anabaena* sensory rhodopsin (*A*SR) is one of the new type 1 rhodopsins. Its gene was identified in the genome of the freshwater cyanobacterium *Anabaena* (*Nostoc*) sp. PCC7120 (18). A 14-kDa soluble protein is encoded under the same promoter with the opsin and is believed to be a cytoplasmic messenger in the sensory transduction chain initiated by photoexcitation of *A*SR (7). *A*SR signaling to a soluble cytoplasmic transducer is more analogous to visual pigment function than to that of haloarchaeal SRI and SRII, which relay signals to integral membrane transducers.

Submitted July 19, 2006, and accepted for publication September 8, 2006.

Address reprint requests to John L. Spudich, Center for Membrane Biology, University of Texas, Medical School, Houston, TX 77030. Tel.: 713-500-5473; Fax: 713-500-0545; E-mail: john.l.spudich@uth.tmc.edu.

0006-3495/06/12/4519/09 $2.00

doi: 10.1529/biophysj.106.093641

Here we report that the C-terminal extension plays an important role in the photochemical processes of the *A*SR protein, as in visual pigments. Truncation of this part of *A*SR causes dramatic changes in charge movements. In particular, the vectoriality of proton transfer from the Schiff base during M formation is inverted from outwardly directed to toward the cytoplasm. Also charge movements occurring during L-intermediate formation (which precedes Schiff base deprotonation) are altered by truncation. These effects are difficult to detect with conventional UV-Vis kinetic absorption spectroscopy, which is insensitive to charge vectoriality.

METHODS

Plasmid construction

Full-length *Anabaena* opsin ($ASR_{1–261}$) was cloned into pET15b modified using NdeI and NotI restriction sites. Polymerase chain reaction (PCR) was used to obtain a truncated sequence encoding 229 residues ($ASR_{1–229}$). PCR was used to introduce a His_6 tag at the carboxy terminus of the two opsin proteins for protein purification. The constructs were expressed under the plac1 promoter of pMS107 in UT5600 *Escherichia coli* cells. The opsin fragment from pET vector (*Xba*I/*Not*I insert) was ligated into the expression vector pMS107 (18).

Site-directed mutagenesis

The mutations D75E, S86D, and D217N were introduced either by QuickChange site-directed mutagenesis (Stratagene, La Jolla, CA) or by the two-step PCR method (20). All mutagenesis was conducted on full-length and truncated *Anabaena* opsin genes with and without His_6 tags and confirmed by DNA sequencing.

Protein expression and purification

All constructs were transformed into *E.coli* UT5600 for expression. The cells were grown at 37°C to $A_{600} = 0.4–0.5$ and induced with 1 mM IPTG added with 5 μM all-*trans* retinal. Cells were harvested by centrifugation at 4000 *g*. For membrane preparation, cells were resuspended in 50 mM Tris, 300 mM NaCl, pH 7.6 buffer (buffer A) containing 10% glycerol. Resuspended cells were lysed using a microfluidizer, and unlysed cells were removed by centrifugation at 4000× *g*. The membranes were prepared by centrifugation of lysed cells at 150,000× *g* for 1 h. For purification, the protein was extracted using 1% dodecyl maltoside (DDM) in buffer A overnight, followed by centrifugation at 20,000× *g* to remove unextracted material. The protein was loaded on a preequilibrated Ni-NTA agarose column, washed with 20 mM imidazole in buffer B (buffer A with 0.05% DDM), and finally eluted with 250 mM imidazole in buffer B. Eluted protein was concentrated and dialyzed to remove imidazole. All steps were performed at 4°C.

Photoinduced current measurements

E. coli cells, cultured as described above, were washed with distilled water and resuspended in measuring buffer containing 10 mM Tris-HCl, 2 mM NaCl, 0.1 mM $MgCl_2$, and 0.1 mM $CaCl_2$ (pH ~ 7.7). Charge movements within *A*SR molecules were detected by measurements of laser flash-induced currents in suspensions of *E. coli* cells expressing the pigment or its mutated versions. This approach is based on a light-focusing effect through the virtually transparent cell body (see Sineshchekov and Spudich (21) for details). Briefly, suspensions of cells were flashed along the line between platinum electrodes by Nd:YAG Minilite laser (532 nm, 6-ns pulse; Continuum, Santa Clara, CA). Essentially equal quanta of light should be absorbed on both halves of the cell membrane because of the low absorption of light within the cell. Nevertheless, the projection of elementary currents through the uniformly excited molecules on the illuminated side of the cell on the line between the measuring electrodes is smaller than the projection on the opposite side, where light beams are concentrated at the center. The difference in the oppositely directed currents caused by the excitation light was detected by a low-noise current amplifier 428 (Keithley Instruments, Cleveland, OH) with 5-μs rise time. Signals were digitized by a DIGIDATA 1320A at 2 or 4 μs/point and stored in a PC using the Clampex 9.0 program (both from Axon Instruments, Foster City, CA), and 40–120 transients obtained with a 10-s flash interval were averaged. Small flash artifacts were recorded using a suspension of *E. coli* cells not expressing pigment and were subtracted from the current signals. To measure voltage signals reflecting the overall charge movement, current traces were time-integrated using the same program. Data were reduced with logarithmically increasing numbers of averaging points along the time axis and analyzed by the Origin 7.0 program (OriginLab, Northampton, MA).

Absorption and flash photolysis

Flash-induced absorption changes were acquired in parallel with a laboratory-constructed cross-beam flash-photolysis system under conditions identical to those of the current measurements except for a higher intensity of the Nd-YAG pulse laser (Continuum, Surelite I, Santa Clara, CA) as described (22). Absorption spectra were measured with a Cary 4000 UV-Vis Spectrophotometer (Varian, Palo Alto, CA) using an integrating sphere.

RESULTS

C-terminal truncation has only minor effects on *A*SR absorption and photochemistry. The full-length ($ASR_{1–261}$) and C-terminally truncated ($ASR_{1–229}$) versions of *A*SR used in this study are schematically shown in Fig. 1. The expression level of $ASR_{1–261}$ in *E. coli* cells was ~40% of that of $ASR_{1–229}$. A similar reduced level of expression of full-length versus truncated versions of all tested mutants was observed (see below).

The full-length *A*SR revealed the same unusual light-dark adaptation as was reported earlier in the truncated pigment (22). The light-adapted form of *A*SR has mostly 13-*cis*/15-syn retinal, whereas dark adaptation leads to its thermal conversion to the all-*trans*/15-anti form (22,23). The two isomeric forms of *A*SR have different absorption spectra and undergo mutual light-induced photoconversion. Thus, their ratio depends on the wavelength of illumination, providing a potential mechanism for single-pigment color sensing (19,22). Nearly identical dark-adapted minus light-adapted difference absorption spectra of freshly purified $ASR_{1–261}$ and $ASR_{1–229}$ (Fig. 2 *A*) showed that the truncation does not affect absorption properties of either the all-*trans* or the 13-*cis* form of pigment, but the rate of dark adaptation was ~1.5-fold slower in the full-length compared to the truncated pigment (Fig. 2 *B*). The photocycle rate of the purified full-length *A*SR was ~20% faster than that of the truncated pigment (Fig. 2 *C*). As we reported earlier, the photocycle of truncated *A*SR significantly slows down in intact *E. coli* cells, as compared to that of purified pigment in detergent

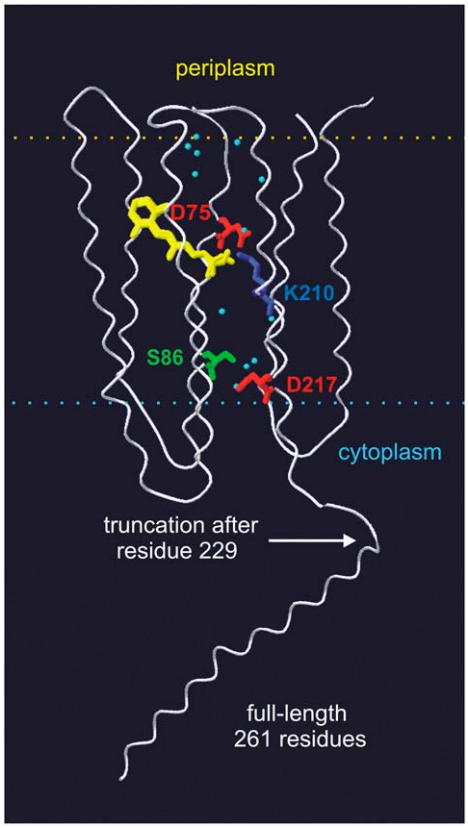

FIGURE 1 Representation of the full-length *A*SR. Transmembrane helices (*white*), retinal (*yellow*), and key residues and water molecules (*cyan*) are shown according to the crystal structure of the truncated protein (19). The structure of the cytoplasmic 35 residues beyond residue 226 is unknown and shown arbitrary as an α-helical extension.

(22). The full-length *A*SR showed a much stronger deceleration of the photocycle in intact cells. Consequently, in intact *E. coli* cells, the peak and decay times of the flash-induced absorption changes were about twofold longer in the full-length *A*SR than in the truncated pigment (Fig. 2 *D*).

From the above UV-Vis spectroscopy and flash photolysis results, we conclude that the full-length and C-terminally truncated versions of *A*SR show only quantitative differences in their optical characteristics, which were more pronounced in intact cells than in detergent.

C-terminal truncation has major effects on charge movements in the *A*SR photocycle. In contrast, we observed a dramatic qualitative effect of the C-terminal truncation on the photoinduced electrical charge movement in *E. coli* cells. Experimental current signals are better suited for analysis of fast electrical events (Fig. 3 *A*), whereas computed photovoltaic curves (time integrals of the currents, Fig. 3 *B*) reflect the overall charge movement within the rhodopsin molecule and are more informative than current signals over an extended timescale (24,25). The charge movement in the truncated *A*SR comprises several kinetic components (Fig. 3 *B*). The first component (τ of several microseconds) reflects charge movement related to the formation of the K intermediate, unresolved in our measurements (26). We used the amplitude of this component as a point for normalization of current and charge signals to compensate for differences in the expression levels of the full-length and the truncated *A*SR. A component with $\tau \sim 40$–100 μs correlates with the time constant of L intermediate formation in purified *A*SR (22). A slow (τ of several milliseconds) component corresponds to the time window of M intermediate formation, which includes Schiff base deprotonation. In many cases, it can be decomposed into a minor submillisecond and a major several-millisecond phase, which fits well to the biphasic formation of the M intermediate reported earlier (22). As we have shown in a previous study (21), in the truncated version of *A*SR, all phases of the charge movement up to the peak time of the M formation are directed toward the cytoplasmic side of the membrane (Fig. 3 *B*).

The charge movement detected in the native full-length pigment reveals similar kinetic components as found in the truncated *A*SR. However, only the fastest unresolved component, related to the formation of the K intermediate, has a negative (inwardly directed) sign in the full-length pigment (Fig. 3 *B*). The later components have the outward direction, in contrast to the respective signal components in the truncated *A*SR.

The effect of truncation is most evident in the difference curve between charge movement in full-length and truncated versions of the pigment (Fig. 3 *C*, *solid line*). The difference signal comprises two main components with peaks $\sim$100 μs and $>$10 ms time ranges. The close kinetic match of the millisecond charge difference signal with the kinetics of M formation and decay (monitored by absorbance changes at 400 nm) shows that truncation inverts the direction of proton movement associated with the Schiff base deprotonation.

A fast component of the difference signal peaking at $\sim$100 μs precedes Schiff base deprotonation and fits well to the kinetics of L intermediate formation (monitored by absorbance changes at 460 nm on Fig. 3 *C*). Charge motion associated with rearrangements of several residues, retinal, and bound water contributes to photocurrent during L formation in bacteriorhodopsin (BR) (27,28). The dependence of the fast charge movement in *A*SR on the presence of the full-length C-terminus shows that the structures of either the unphotolyzed state, the L-intermediate, or both are different in full-length and truncated pigments.

Although the kinetics of the millisecond charge movement correlates well with M formation in both the full-length and the truncated *A*SR, additional slower components are superimposed on the Schiff base deprotonation signals in the later part of the photocycle (Fig. 4). Their chemical origin is not clear from the available data.

The inversion of charge movement vectoriality by truncation is not influenced by C-terminal His_6 tags. It has been reported that His_6 tags modify the photochemistry of visual rhodopsins (9). To test the possibility that this sequence,

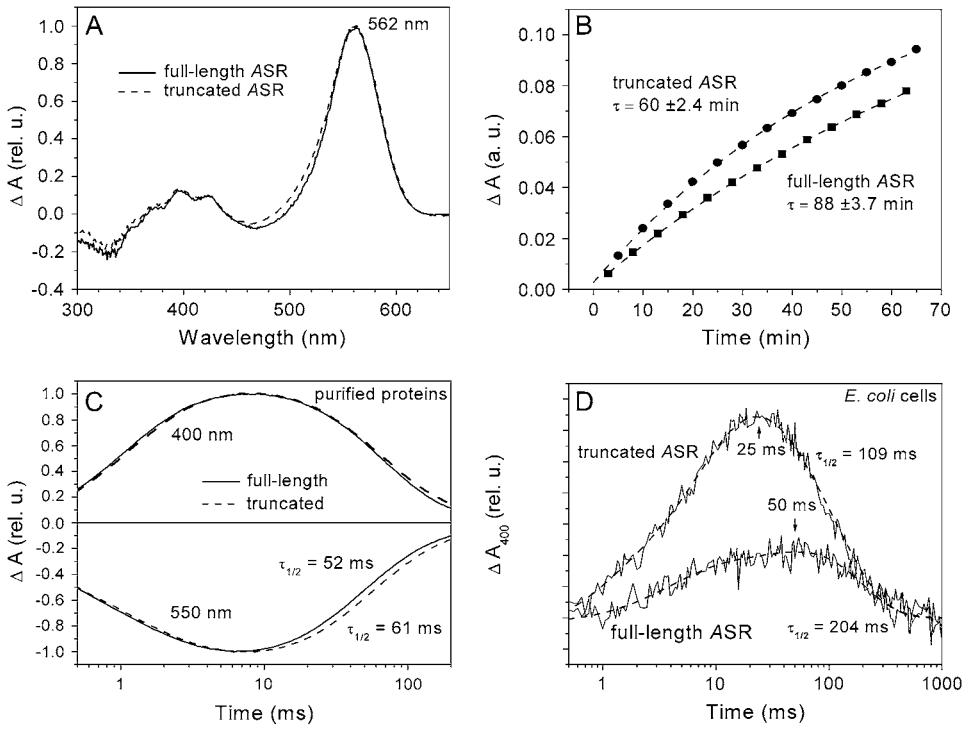

FIGURE 2 Comparison of spectroscopic and photochemical properties of full-length and truncated *A*SR. (*A*) Difference absorption spectra of dark-adapted minus light-adapted purified pigments in detergent. (*B*) Kinetics of dark adaptation in purified pigments. Absorption changes were normalized to the absorption of dark-adapted samples. (*C*) Laser flash induced absorption changes of purified pigments at different wavelengths, monitoring the unphotolyzed state (550 nm) and M intermediate (400 nm). (*D*) Formation and decay of M intermediate pigments in intact *E. coli* cells.

located in the truncated version close to the opening of the cytoplasmic channel, contributes to the inversion of charge movements, we expressed His_6-tag-free full-length and truncated *A*SR. The inverting effect of truncation on charge movements was observed both in the presence and absence of the His_6 tags (cf. Fig. 3 and Fig. 4). Thus, the inversion of the direction of charge and proton movements is caused specifically by the truncation of the C terminus and is independent of the His_6 tag.

Mutation of Asp^{217} to Asn inverts the charge movement in truncated $ASR_{1–229}$. A recent time-resolved FTIR study of the truncated *A*SR showed that Asp^{217}, ~15 Å to the cytoplasmic side of the membrane from the Schiff base, acts as a proton acceptor (29). These data are in accordance with the cytoplasmic direction of charge movement in the truncated *A*SR reported earlier (21). Here we used site-directed mutagenesis to probe for the role of this residue in the photoinduced charge movement within *A*SR. In the truncated *A*SR, neutralization of this residue by the D217N mutation inverted the direction of charge movement from negative (inwardly directed) to positive, so that the mutated truncated *A*SR behaved similarly to the full-length wild-type pigment (Fig. 5 *A*). At least three kinetic components of difference signals between the truncated and full-length versions of the wild-type *A*SR and between the truncated wild-type pigments and truncated D217N mutant pigment are very similar, although the millisecond component is more pronounced in the case of the D217N mutation (Fig. 5 *B*).

In the full-length version of the D217N mutant pigment, the outwardly directed charge movement is further increased in amplitude compared to the truncated version of the mutant. However, the effect of the truncation in the D217N mutant is relatively larger on the fast ($\tau < 100$ μs) component, which corresponds to the L intermediate formation in the purified protein and precedes deprotonation of the Schiff base. The absence of significant effects of the D217N mutation on the charge movement on the millisecond time scale in the full-length *A*SR, as opposed to dramatic changes induced by this mutation in the truncated version, indicates that Asp^{217} acts as a proton acceptor only in the truncated pigment. This result is in accord with the observation from an FTIR study that no aspartate protonation signal occurs in the full-length protein, $ASR_{1–261}$ (23), unlike the case of $ASR_{1–229}$ (29).

Flash-induced absorption changes of D217N mutants also differed between the full-length and truncated versions of *A*SR. As noted above, in intact *E. coli* cells a slower decay of the M intermediate was detected in the wild-type full-length version of *A*SR than in the truncated version (Fig. 2 *D*). The D217N mutation increased the lifetime of the M intermediate of the truncated pigment nearly threefold in intact *E. coli* cells, in accordance with a similar effect in purified truncated pigment (29). In contrast to the wild type, the full-length version of this mutant showed a significantly faster decay of the M intermediate than the truncated version (Fig. 5 *C*). As a result, the lifetimes of the M intermediates were very similar (~200 ms) in the full-length versions of the wild type and the D217N mutant, which further confirms that Asp^{217} does not play an important role in photochemistry of the full-length (native) *A*SR.

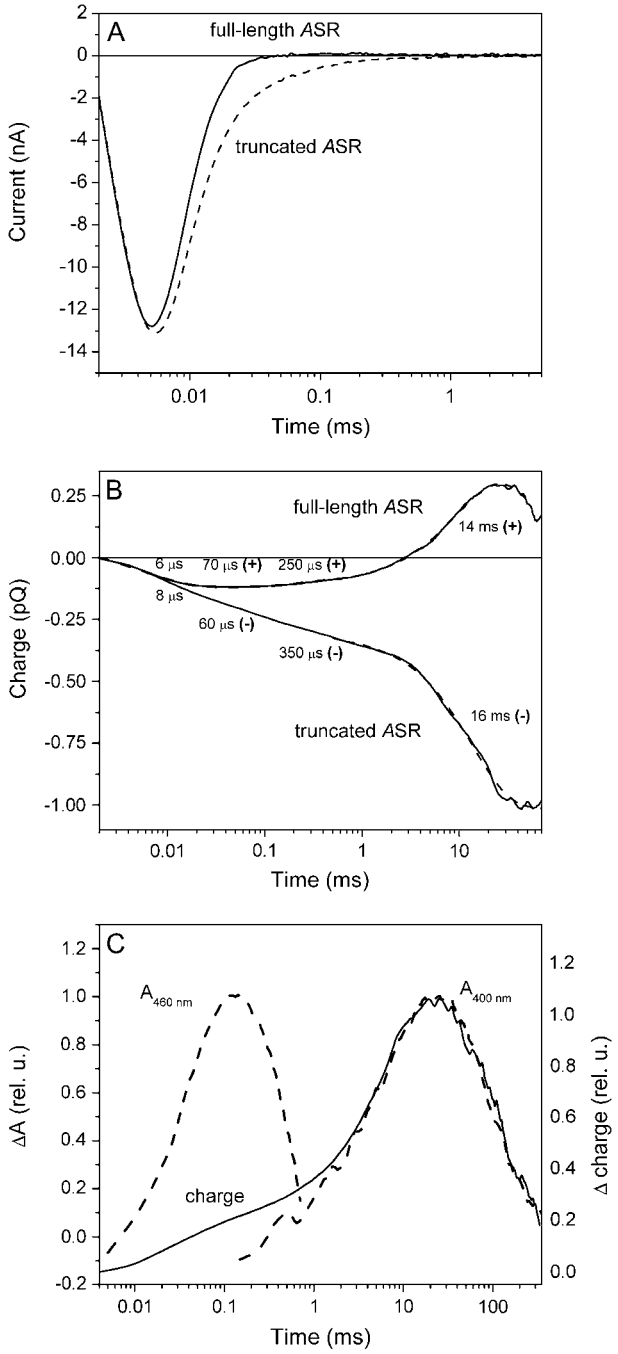

FIGURE 3 (*A*) Laser flash–induced electric currents generated by full-length and truncated *A*SR in suspension of intact *E. coli* cells (for details of the method, see Sineshchekov and Spudich (21)). (*B*) Time integrals of current signals reflecting overall charge movement in full-length and truncated *A*SR. Outwardly directed positive charge movement corresponds to an upward slope of the curves. (*C*) Correlation of difference charge signal between full-length and truncated versions of *A*SR (*solid line*) with absorption changes (*dashed lines*) at wavelength characteristic for L- and M-like intermediates (460 nm and 400 nm, respectively). Because of the high light scattering of cell suspensions, L formation was measured in purified pigment.

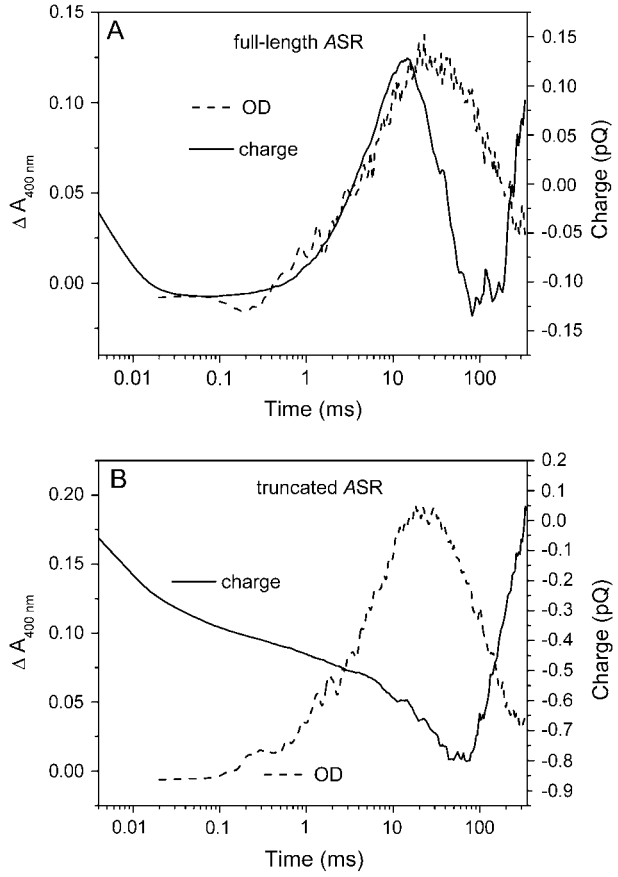

FIGURE 4 Charge movement (*solid lines*) and M intermediate kinetics (*dashed lines*) in full-length (*A*) and truncated (*B*) *A*SR without C-terminal His_6 tags.

Mutation of Asp^{75} to Glu reverses the inverted vectoriality of charge movement in truncated $ASR_{1–229}$. Asp^{75} in the primary sequence of *A*SR corresponds to the Schiff base counterion and proton acceptor Asp^{85} in BR. The position of Asp^{75} on the extracellular side of the membrane with respect to the Schiff base has been confirmed by x-ray crystallography, and its proximity argues that it serves as the Schiff base counterion as in BR and SRII (19). The positive sign of the voltage signal in full-length *A*SR indicates that the proton moves in the direction of this residue, as occurs in proton-pumping rhodopsins and SRII (21,27). In *A*SR the rate of this charge movement, as well as the rate of M intermediate formation, is very slow compared to that of other microbial rhodopsins. This indicates that Asp^{75} does not serve as a strong proton acceptor even in the full-length native *A*SR in which the charge moves outward. The mutation of Asp^{75} to Glu in the truncated *A*SR leads to the appearance of a fast outwardly directed current of large amplitude, typical for proton transfers to the counterion carboxylate in other rhodopsins (Fig. 6 *A*). The full-length version of this D75E mutant also demonstrates a similar acceleration of the outward photocurrent and charge movement (Fig. 6, *A* and *B*). In both full-length and truncated pigments, the D75E mutation

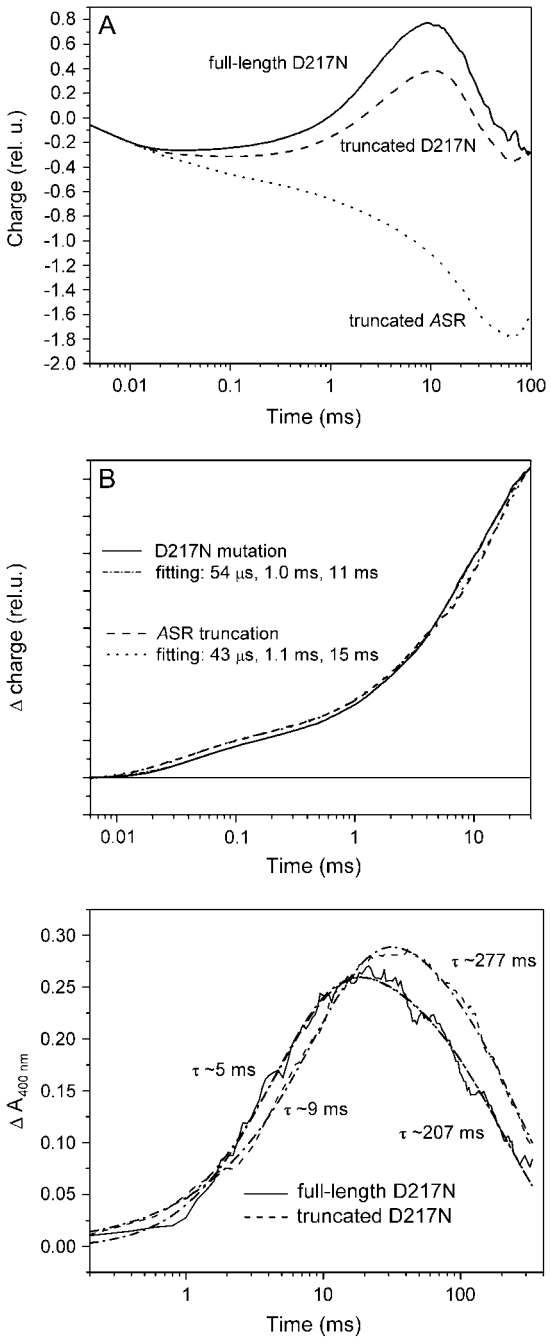

FIGURE 5 (*A*) Charge movement in full-length (*solid line*) and truncated (*dashed line*) D217N mutant. Charge movement in truncated wild-type *A*SR is given for comparison (*dotted line*). (*B*) Normalized difference signals reflecting the effect of D217N mutation of truncated *A*SR (truncated D217N minus truncated ASR, *black line*), and the effect of truncation in wild-type *A*SR (full-length *A*SR minus truncated *A*SR, *dashed line*). (*C*) Effect of truncation on the M intermediate kinetics in the D217N mutant.

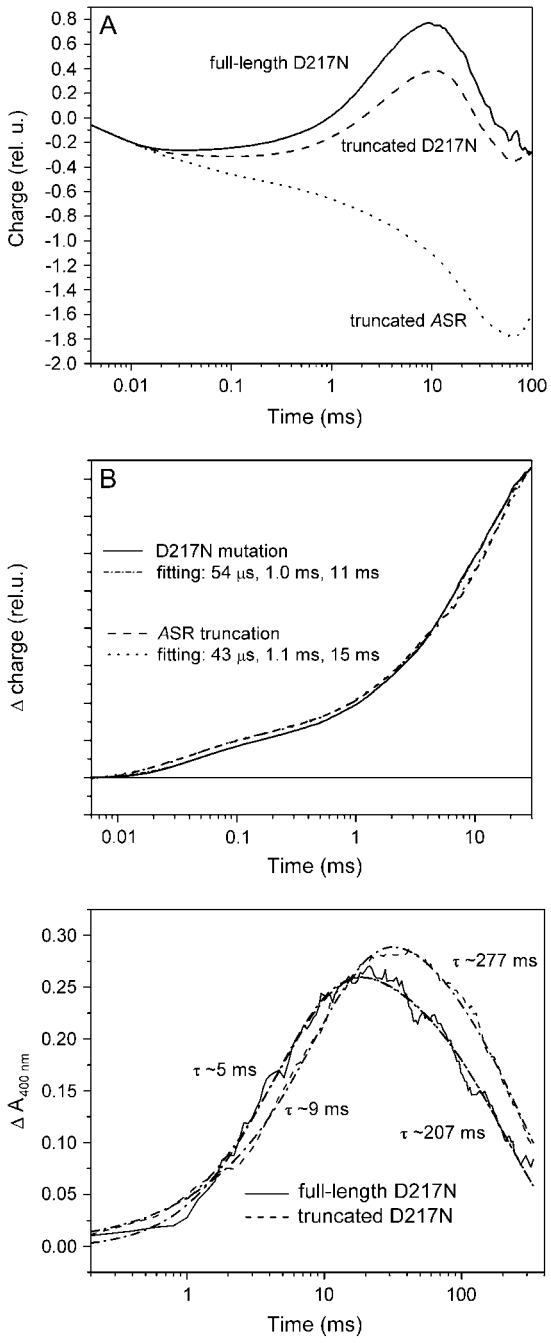

FIGURE 6 Effect of mutation of Asp^{75} in *A*SR (a homolog of the proton acceptor Asp^{85} in BR) to glutamate. Photocurrents (*A*) and charge movement (*B*) in the full-length (*solid lines*) and the truncated (*dashed lines*) D75E mutant (signals in wild-type *A*SR are given for comparison by *dotted and dashed-dotted lines*). (*C*) M intermediate kinetics in truncated wild-type *A*SR and truncated D75E mutants in intact *E. coli* cells.

brings about a corresponding acceleration of M intermediate formation (Fig. 6 *C*).

Mutation of Ser^{86} to Asp inverts the direction of late charge movement in full-length and truncated D75E mutants. The lack of proton-pumping activity in *A*SR may be caused by the lack of a strong Schiff base proton acceptor and/or the absence of a Schiff base proton donor because a nonprotonatable residue, Ser^{86}, in *A*SR is at the position in helix C homologous to that of the Schiff base proton donor,

Asp^{96}, in BR. To test whether the Schiff base would be reprotonated from this position when the strong proton acceptor Glu^{75} is present in the BR Asp^{85} position, we constructed full-length and truncated versions of the double mutant D75E/S86D. Not only does the double mutant not show an increase in outwardly directed charge transfer but, unexpectedly, the S86D mutation inverted the late phases of charge movement to the cytoplasmic direction (Fig. 7 *A*). When this mutation was introduced into full-length versions of wild-type *A*SR, the outwardly directed proton movement was greatly suppressed, or even inverted to the cytoplasmic direction. Only the millisecond component of charge movement is affected by this mutation (Fig. 7 *B*). These results indicate that the introduction of potential negative charge in the *A*SR cytoplasmic channel is sufficient to influence the efficiency and even the direction of proton movement.

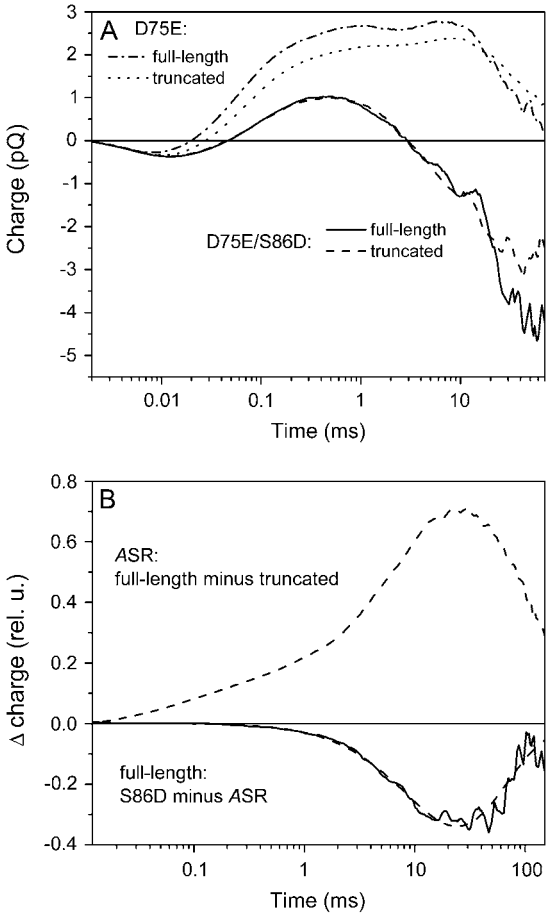

FIGURE 7 Effect of substituting a protonatable residue at the *A*SR Ser^{86} position (homologous to the Schiff base proton donor in BR, Asp^{96}). (*A*) Inversion of the late phases of proton movement in the full-length (*solid line*) and truncated (*dashed line*) double mutant D75E/S86D. Charge movements in single D75E mutants are given for comparison (*dashed-dotted and dotted lines* for full-length and truncated, respectively). (*B*) Comparison of the effect of truncation in the wild-type *A*SR (*dashed line*) with the effect of S86D mutation in the full-length *A*SR (*solid line*).

DISCUSSION

The above results show that the direction of charge movement in the photochemical reaction cycle of *A*SR leading to formation of the L and M intermediates is regulated by the hydrophilic C-terminal portion of the protein. In particular, the proton transfer from the retinylidene Schiff base located in the membrane-embedded interior of the protein is inverted from outwardly directed to inwardly directed when the cytoplasmic C-terminal portion is truncated. Apparently the proton transfer direction from the Schiff base is variable in the ASR protein and able to be changed by distant modifications. Confirming this, site-specific mutations distant from the photoactive site residues on the cytoplasmic side of the protein that introduce (S96D) or remove (D217N) a potential negative charge favor or disfavor, respectively, a cytoplasmic direction of proton release from the Schiff base.

Our interpretation is that the photoactive site and the cytoplasmic domain of the protein are in communication, likely through a network of hydrogen bonds connecting the cytoplasmic residues and the retinylidene Schiff base, which may be modified by minor and/or distant changes in the molecule. A crystal structure of *A*SR (truncated) shows numerous hydrophilic residues on the cytoplasmic side networked by water molecules, providing such a connection from the photoactive site to the cytoplasmic surface (19). The existence of such strong cytoplasmic/photoactive site coupling in *A*SR is not evident in haloarchaeal phototaxis receptors SRI and SRII. Supporting our interpretation, the cytoplasmic half-channel in SRII is highly hydrophobic according to its crystal structure (30).

The difference between *A*SR and haloarchaeal sensory rhodopsins may be correlated with their different signal relay mechanisms. SRI and SRII signal through integral membrane transducers (31) and have a membrane-embedded receptor-transducer interface (32), whereas *A*SR most probably initiates a signal transduction pathway by interaction with the 14-kDa cytoplasmic transducer. The transducer is a water-soluble protein that presumably interacts with cytoplasmic extensions of *A*SR, which are comprised of its cytoplasmic loops and the C-terminal tail. In support of a contribution of the C-terminal tail, microcalorimetric measurements show an about fourfold greater affinity of the 14-kDa protein for the full-length version of *A*SR than for the truncated form (V. D. Trivedi and J. L. Spudich, unpublished data).

C-terminal truncation affects at least two kinetically separated processes in ~100 μs and several-millisecond timescales. Inversion of the charge movement in the millisecond timescale and the matching kinetics of the slower difference charge signal with the kinetics of the M intermediate show that the direction of proton movement following the Schiff base deprotonation is opposite in truncated and full-length pigments (Figs. 3 and 4). The inwardly directed movement

in the truncated *A*SR is reversed by the D217N mutation (Fig. 5 *A*), consistent with it serving as a proton acceptor in the truncated pigment (29). In the full-length *A*SR, the direction of proton movement is toward the extracellular side of the membrane (Figs. 3 *B* and 4 *B*), which means that Asp^{217}, located to the cytoplasmic side of the membrane with respect to the Schiff base, does not serve as a proton acceptor in the native pigment, in accord with the lack of a carboxylate protonation signal in FTIR spectra (23). This is confirmed by the very small effect of D217N mutation on the charge movement and photocycle rate of the full-length pigment. Consequently, one does not expect a signaling role of the cytoplasmic proton shuttling identified recently in the truncated protein (29), at least during M intermediate formation, because such shuttling does not take place in the native full-length *A*SR at this stage. However, the accessibility of the released Schiff base proton to a cytoplasmic channel may appear in the later part of the cycle, similar to a switch of the Schiff base accessibility from the extracellular to a cytoplasmic channel, which occurs in late M in BR (5).

The proton transfer ~15 Å from the Schiff base to Asp^{217} in truncated *A*SR correlates with a high-amplitude inwardly directed charge movement in this time window. We attribute this long-distance movement to the extensive hydrogen-bonded network of water molecules in the hydrophilic cytoplasmic channel evident in the crystal structure of truncated *A*SR (19). According to our data, Asp^{217} becomes inaccessible to the Schiff base proton in the full-length pigment. This may be because of the disruption of the hydrogen-bonded network and, hence, a different structure of the cytoplasmic channel in the native pigment.

Truncation not only makes Asp^{217} an artificial proton acceptor but also modifies the vicinity of the retinal involved in L intermediate formation in the hundred-microsecond time range. Although the direction of proton movement in the D217N mutant does not depend on truncation, differences affecting the microsecond component are still observed between full-length and truncated versions (Fig. 5). Hydrogen-bonded water molecules are involved in structural rearrangements and charge movement during L formation in BR (27,28). Therefore, our finding may be relevant to analysis of FTIR data on the state of hydrogen-bonded water molecules (33,34), since there is expected to be a structural difference between full-length and truncated *A*SR.

The M formation and associated charge movement are slow in the full-length as well as in truncated versions of *A*SR compared to known proton-pumping rhodopsins. Therefore, Asp^{75} does not serve as a strong proton acceptor even in the full-length *A*SR, although we cannot fully exclude its participation in Schiff base deprotonation. This is consistent with the lack of an Asp^{75} protonation signal during M formation from FTIR of photoactivated *A*SR (23). The Schiff base proton may instead be accepted by networked water molecules at the extracellular side of the Schiff base. Creation of an active primary carboxylate acceptor in *A*SR is achieved by the mutation D75E, as indicated by the appearance of fast outward charge movement of large amplitude, characteristic of proton transfer to the nearby Schiff base counterion in other microbial rhodopsins, in both the full-length and the truncated versions of the pigment (Fig. 6). Similar acceleration of M formation caused by Asp-to-Glu mutation of the counterion has been reported earlier for BR (35).

Two possibilities for *A*SR signaling were suggested earlier (22). The first is that the ratio of the unphotolyzed forms with *trans*- and *cis*-retinals, which not only changes greatly on light and dark adaptation but also depends on light quality, may modulate a photobiological function. Alternatively, the long-lived M intermediate may serve as a signaling form. The strong coupling between the C-terminal region and processes involved in M formation reported here favors the second possibility because it suggests that M formation in turn can cause conformational changes in the cytoplasmic C-terminal extension and modulate its interaction with the water-soluble transducer.

The importance of extramembranous regions of rhodopsin molecules to their photochemistry and function may also be expected in other newly found microbial rhodopsins. Recently, we reported strong deceleration of the photocycle by truncation of the extracellular N-terminal of rhodopsin from the cryptophyte alga *Guillardia* (36). In *Chlamydomonas* sensory rhodopsins (CSRA and CSRB), the length of the C-terminal parts of the molecules exceeds that of the seven transmembrane helices (17,37–39). The functional roles of the C-terminal domains have not been elucidated. It has been reported that they are not necessary for the channel activity of these pigments when heterologously expressed (37,38). However, the signal transduction pathway for *Chlamydomonas* phototaxis involves a biochemical amplification cascade (40,41), and the C-terminal rhodopsin domains may relay the signal to this cascade. Alternatively, the C-terminal domain may control the photochemical activity of the molecule. Therefore, in this case also, one might expect coupling between the photoactive site and C-terminal domains, as reported here for *A*SR.

The authors are grateful to Kevin Ridge for discussion and comments on the manuscript and to Elena Govorunova for help in manuscript preparation.

This work was supported by the Russian Foundation for Basic Research grant 05-04-48805 (to O.A.S.), and by National Institutes of Health grant R37GM27750 and the Robert A. Welch Foundation (to J.L.S.).

REFERENCES

1. Spudich, J. L., C. S. Yang, K. H. Jung, and E. N. Spudich. 2000. Retinylidene proteins: structures and functions from archaea to humans. *Annu. Rev. Cell Dev. Biol.* 16:365–392.
2. Ebrey, T., and Y. Koutalos. 2001. Vertebrate photoreceptors. *Prog. Retin. Eye Res.* 20:49–94.
3. Spudich, J. L., and K. H. Jung. 2005. Microbial rhodopsins: phylogenetic and functional diversity. *In* Handbook of Photosensory Receptors. W. R. Briggs and J. L. Spudich, editors. Wiley-VCH, Weinheim, Germany. 1–24.

4. Terakita, A. 2005. The opsins. *Genome Biol.* 6:213.1–213.9
5. Luecke, H., and J. K. Lanyi. 2003. Structural clues to the mechanism of ion pumping in bacteriorhodopsin. *Adv. Protein Chem.* 63:111–130.
6. Brown, L. S., and K. H. Jung. 2006. Bacteriorhodopsin-like proteins of eubacteria and fungi: the extent of conservation of the haloarchaeal proton-pumping mechanism. *Photochem. Photobiol. Sci.* 5:538–546.
7. Spudich, J. L. 2006. The multitalented microbial sensory rhodopsins. *Trends Microbiol.* 14:480–487.
8. Ridge, K. D., N. G. Abdulaev, M. Sousa, and K. Palczewski. 2003. Phototransduction: crystal clear. *Trends Biochem. Sci.* 28:479–487.
9. Janssen, J. J., P. H. Bovee-Geurts, M. Merkx, and W. J. DeGrip. 1995. Histidine tagging both allows convenient single-step purification of bovine rhodopsin and exerts ionic strength-dependent effects on its photochemistry. *J. Biol. Chem.* 270:11222–11229.
10. Ovchinnikov, Y. A., N. G. Abdulaev, A. V. Kiselev, L. A. Drachev, A. D. Kaulen, and V. P. Skulachev. 1986. The water-exposed C-terminal sequence of bacteriorhodopsin does not affect H^+ pumping. *FEBS Lett.* 194:16–20.
11. Olson, K. D., and J. L. Spudich. 1993. Removal of the transducer protein from sensory rhodopsin I exposes sites of proton release and uptake during the receptor photocycle. *Biophys. J.* 65:2578–2585.
12. Yang, C. S., and J. L. Spudich. 2001. Light-induced structural changes occur in the transmembrane helices of the *Natronobacterium pharaonis* HtrII transducer. *Biochemistry.* 40:14207–14214.
13. Ferrando-May, E., B. Brustmann, and D. A. Oesterhelt. 1993. A C-terminal truncation results in high-level expression of the functional photoreceptor sensory rhodopsin I in the archaeon *Halobacterium salinarium*. *Mol. Microbiol.* 9:943–953.
14. Sharma, A. K., J. L. Spudich, and W. F. Doolittle. 2006. Microbial rhodopsins: functional versatility and genetic mobility. *Trends Microbiol.* 14:463–469.
15. Spudich, J. L., and R. A. Bogomolni. 1984. Mechanism of color discrimination by a bacterial sensory rhodopsin. *Nature.* 312:509–513.
16. Hoff, W. D., K. H. Jung, and J. L. Spudich. 1997. Molecular mechanism of photosignaling by archaeal sensory rhodopsins. *Annu. Rev. Biophys. Biomol. Struct.* 26:223–258.
17. Sineshchekov, O. A., K. H. Jung, and J. L. Spudich. 2002. Two rhodopsins medicate phototaxis to low- and high-intensity light in *Chlamydomonas reinhardtii*. *Proc. Natl. Acad. Sci. USA.* 99:8689–8694.
18. Jung, K. H., V. D. Trivedi, and J. L. Spudich. 2003. Demonstration of a sensory rhodopsin in eubacteria. *Mol. Microbiol.* 47:1513–1522.
19. Vogeley, L., O. A. Sineshchekov, V. D. Trivedi, J. Sasaki, J. L. Spudich, and H. Luecke. 2004. *Anabaena* sensory rhodopsin: a photochromic color sensor at 2.0 A^o. *Science.* 306:1390–1393.
20. Ho, S. N., H. D. Hunt, R. M. Horton, J. K. Pullen, and L. R. Pease. 1989. Site-directed mutagenesis by overlap extension using the polymerase chain reaction. *Gene.* 77:51–59.
21. Sineshchekov, O. A., and J. L. Spudich. 2004. Light-induced intramolecular charge movements in microbial rhodopsins in intact *E. coli* cells. *Photochem. Photobiol. Sci.* 3:548–554.
22. Sineshchekov, O. A., V. D. Trivedi, J. Sasaki, and J. L. Spudich. 2005. Photochromicity of *Anabaena* sensory rhodopsin, an atypical microbial receptor with a *cis*-retinal light-adapted form. *J. Biol. Chem.* 280:14663–14668.
23. Bergo, V. B., M. Ntefidou, V. D. Trivedi, J. J. Amsden, J. M. Kralj, K. J. Rothschild, and J. L. Spudich. 2006. Conformational changes in the photocycle of *Anabaena* sensory rhodopsin: Absence of the Schiff base counterion protonation signal. *J. Biol. Chem.* 281:15208–15214.
24. Ludmann, K., C. Gergely, A. Dér, and G. Váró. 1998. Electric signals during the bacteriorhodopsin photocycle, determined over a wide pH range. *Biophys. J.* 75:3120–3126.
25. Oroszi, L., A. Dér, and P. Ormos. 2002. Theory of electric signals of membrane proteins in three dimensions. *Eur. Biophys. J.* 31:136–144.
26. Dér, A., and L. Keszthelyi. 2001. Charge motion during the photocycle of bacteriorhodopsin. *Biochemistry (Mosc.).* 66:1234–1248.
27. Lanyi, J. K. 2004. What is the real crystallographic structure of the L photointermediate of bacteriorhodopsin? *Biochim. Biophys. Acta.* 1658:14–22.
28. Tóth-Boconádi, R., A. Dér, S. G. Taneva, and L. Keszthelyi. 2006. Excitation of the L intermediate of bacteriorhodopsin: electric responses to test x-ray structures. *Biophys. J.* 90:2651–2655.
29. Shi, L., S. R. Yoon, A. G. Bezerra, Jr., K. H. Jung, and L. S. Brown. 2006. Cytoplasmic shuttling of protons in *Anabaena* sensory rhodopsin: implications for signaling mechanism. *J. Mol. Biol.* 358:686–700.
30. Luecke, H., B. Schobert, J. K. Lanyi, E. N. Spudich, and J. L. Spudich. 2001. Crystal structure of sensory rhodopsin II at 2.4 angstroms: insights into color tuning and transducer interaction. *Science.* 293:1499–1503.
31. Zhang, X. N., J. Zhu, and J. L. Spudich. 1999. The specificity of interaction of archaeal transducers with their cognate sensory rhodopsins is determined by their transmembrane helices. *Proc. Natl. Acad. Sci. USA.* 96:857–862.
32. Gordeliy, V. I., J. Labahn, R. Moukhametzianov, R. Efremov, J. Granzin, R. Schlesinger, G. Büldt, T. Savopol, A. J. Scheidig, J. P. Klare, and M. Engelhard. 2002. Molecular basis of transmembrane signalling by sensory rhodopsin II-transducer complex. *Nature.* 419:484–487.
33. Furutani, Y., A. Kawanabe, K. H. Jung, and H. Kandori. 2005. FTIR spectroscopy of the all-*trans* form of *Anabaena* sensory rhodopsin at 77 K: hydrogen bond of a water between the Schiff base and Asp75. *Biochemistry.* 44:12287–12296.
34. Kawanabe, A., Y. Furutani, K. H. Jung, and H. Kandori. 2006. FTIR study of the photoisomerization processes in the 13-*cis* and all-*trans* forms of *Anabaena* sensory rhodopsin at 77 K. *Biochemistry.* 45:4362–4370.
35. Heberle, J., D. Oesterhelt, and N. A. Dencher. 1993. Decoupling of photo- and proton cycle in the Asp85 Glu mutant of bacteriorhodopsin. *EMBO J.* 12:3721–3727.
36. Sineshchekov, O. A., E. G. Govorunova, K. H. Jung, S. Zauner, U.-G. Maier, and J. L. Spudich. 2005. Rhodopsin-mediated photoreception in Cryptophyte flagellates. *Biophys. J.* 89:4310–4319.
37. Nagel, G., D. Ollig, M. Fuhrmann, S. Kateriya, A. M. Musti, E. Bamberg, and P. Hegemann. 2002. Channelrhodopsin-1: a light-gated proton channel in green algae. *Science.* 296:2395–2398.
38. Nagel, G., T. Szellas, W. Huhn, S. Kateriya, N. Adeishvili, P. Berthold, D. Ollig, P. Hegemann, and E. Bamberg. 2003. Channelrhodopsin-2, a directly light-gated cation-selective membrane channel. *Proc. Natl. Acad. Sci. USA.* 100:13940–13945.
39. Suzuki, T., K. Yamasaki, S. Fujita, K. Oda, M. Iseki, K. Yoshida, M. Watanabe, H. Daiyasu, H. Toh, E. Asamizu, S. Tabata, K. Miura, et al. 2003. Archaeal-type rhodopsins in *Chlamydomonas*: model structure and intracellular localization. *Biochem. Biophys. Res. Commun.* 301:711–717.
40. Sineshchekov, O. A. 1991. Electrophysiology of photomovements in flagellated algae. *In* Biophysics of Photoreceptors and Photomovements in Microorganisms. F. Lenci, F. Ghetti, G. Colombetti, D. P. Häder, and P.-S. Song, editors. Plenum Press, New York. 191–202.
41. Sineshchekov, O. A., and J. L. Spudich. 2005. Sensory rhodopsin signaling in green flagellate algae. *In* Handbook of Photosensory Receptors. W. R. Briggs and J. L. Spudich, editors. Wiley-VCH, Weinheim, Germany. 25–42.